



Experimentation of an adaptive moving mesh finite volume method to solve a Burgers problem with a small diffusion term

Kassiénu Lamien^{1,2,*}, Mamadou Ouédraogo², Somé Longin²

¹Département de mathématiques de l'Institut des Sciences et de Technologie (IST) de l'Ecole Normale Supérieure (ENS), 01 BP 1757 Ouagadougou 01, Burkina Faso

²Laboratoire d'Analyse Numérique, d'Informatique et de Biomathématique, LANIBIO

Received: 13 October 2022 / Received in revised form: 14 December 2022 / Accepted: 26 December 2022

Abstract:

In this paper, we use a particular adaptive moving mesh finite volume method to solve Burger-problem with a small diffusion term. It is well known that the solution of such problem is a wave that spreads and develops a steep front. The main difficulty with the numerical solution of this problem is the computation of this propagating steep front. The purpose in this paper is to point out the efficiency of the use of adaptive moving mesh finite volume method through some comparisons between exact and numerical solutions of this particular problem.

Keywords: Adaptive mesh generation; High-order finite volume method; Hyperbolic conservation laws problems.

1. Introduction

According to Huang and Russell [1]: "moving mesh methods as a whole are still in a relatively early phase of development. Many of them are at the experimental stage, and almost all require further mathematical justification. Rigorous analysis of moving mesh methods for solving time dependent PDEs (Partial Differential Equations) has only been carried out for some very simple model problems to date, and more ways to

improve their efficiency and robustness will no doubt be developed". In this work, we want to improve the method developed by Tang and Tang [2] to solve a Burgers problem with a small diffusion term. There are several other adaptive moving mesh finite volume methods described in [3-11]. Some of them [2, 5, 12, 13] were used to solve some examples of Burger problems with various initial conditions.

*Corresponding author:

Email address: basilelakas@gmail.com (K. Lamien)

The particularity in the present work is about the small diffusion term and the initial conditions.

The two elements which are the diffusion term and the initial condition make it difficult to compute with a classic numerical method based only on domain meshing [1]. Therefore, this form of Burger problem is a good example to apply an adaptive moving mesh method in order to point out its efficiency. The goal of this new technique is to solve this kind of problems with more accuracy using a much lower number of grid points than needed for classical methods.

2. Quick overview of the adaptive moving mesh finite volume method

The considered problem is to find the unknown function $U(x, t)$ on $\Omega =]0, 1[\times]0, 1[$, such as [14, 15]:

$$\frac{\partial U(x, t)}{\partial t} + \frac{\partial f(U(x, t))}{\partial x} = \varepsilon \frac{\partial^2 U(x, t)}{\partial x^2} \quad (1)$$

$$U(x; 0) = Burgers_exact(x; 0)$$

$$U(0; t) = Burgers_exact(0; t)$$

$$U(1; t) = Burgers_exact(1; t)$$

with $\varepsilon = 0.001$, the flux function f and the exact solution given respectively by:

$$f(U(x; t)) = \frac{1}{2} U^2(x, t) \quad (2)$$

and,

$$Burgers_exact(x; t) = \frac{0.1r_1 + 0.5r_2 + r_3}{r_1 + r_2 + r_1} \quad (3)$$

where

$$r_1(x; t) = \exp(-x + 0.5 - 4.95t)/(20\varepsilon)$$

$$r_2(x; t) = \exp(-x + 0.5 - 0.75t)/(4\varepsilon)$$

$$r_3(x; t) = \exp(-x + 0.375)/(2\varepsilon)$$

The problem mentioned above has been solved in [15] using an adaptive moving mesh finite differences method. Another slightly different form by its initial condition has also been solved in [5]. This problem resolution by the chosen adaptive moving mesh finite volume method includes two phases that are mesh generation on the domain and the PDE discretization.

3. Methodology

3.1. Moving mesh generation

At the initial time ($t = 0$) the space interval is subdivided into elementary interval according to the principle of the finite volume method [16, 17]:

$$\left] x_{i-\frac{1}{2}}, x_{i+\frac{1}{2}} \right[, \quad i = \overline{1; N}$$

The nodes resulting from this subdivision form a vector X . For the rest of the time the components of X must change position according to the values of the gradient of solution U . The link between the movement of the nodes and the solution is established by a monitor function ω . This movement of nodes is such as X is considered as follow:

$$X : [0; 1] \rightarrow [a; b]$$

$$\xi \mapsto x(\xi)$$

is solution of Eq. (4), the following mesh-redistribution problem:

$$(\omega X_\xi)_\xi = 0$$

$$X(0) = a \quad (4)$$

$$X(1) = b$$

There are variant forms of the mesh-redistribution equation, as can be seen in [10, 18]. There are also several possible choices for the monitor function [1, 4]. The one we used is defined by:

$$\omega(U) = \sqrt{1 + \alpha \|U_x\|_2^2} \tag{5}$$

with α a positive parameter.

Eq. (5) is approximated for each x_i and at every moment t^n by:

$$\omega(U_i^n) = \sqrt{1 + \alpha \left(\frac{U_{i+1}^n - U_{i-1}^n}{h_i^n} \right)^2} \tag{6}$$

where

$$x_i^n = \frac{1}{2} (x_{i-\frac{1}{2}}^n + x_{i+\frac{1}{2}}^n)$$

and

$$h_i^n = \frac{1}{2} (x_{i+\frac{3}{2}}^n - x_{i+\frac{1}{2}}^n) + (x_{i+\frac{1}{2}}^n - x_{i-\frac{1}{2}}^n) + \frac{1}{2} (x_{i-\frac{1}{2}}^n - x_{i-\frac{3}{2}}^n) \tag{7}$$

According to Tang et Tang [2], the mesh-redistribution equation can be solved by Eq. (8) or by another scheme known as the Gauss-Seidel iteration [2, 3] or also by scheme used by Mackenzie [5].

$$X_{i+1/2}^{n+1} = \varphi_{i+1}^n X_{i+3/2}^n + (1 - \varphi_{i+1}^n - \varphi_i^n) X_{i+\frac{1}{2}}^n + \varphi_i^n X_{i-1/2}^n \tag{8}$$

where

$$\varphi_i^n = \frac{\Delta\tau}{(\Delta\xi)^2} \omega(U_i^n)$$

with $\Delta\tau$ a value such as $\max(\varphi_i^n) \leq \frac{1}{2}$.

In order to obtain better results, it is necessary to perform several iterations of the system formed by Eqs. (8) and (9). Here we have done

15 iterations and taken $\Delta\tau = (h_1^0)^2 \Delta t$, where Δt is the step of time interval.

$$U_i^{n+1} = \frac{x_{i+\frac{1}{2}}^n - x_{i-\frac{1}{2}}^n}{x_{i+\frac{1}{2}}^{n+1} - x_{i-\frac{1}{2}}^{n+1}} U_i^n - \frac{1}{x_{i+\frac{1}{2}}^{n+1} - x_{i-\frac{1}{2}}^{n+1}} \left((CU)_{i+\frac{1}{2}}^n - (CU)_{i-\frac{1}{2}}^n \right) \tag{9}$$

with

$$(CU)_{i+\frac{1}{2}}^n = \frac{C_{i+\frac{1}{2}}}{2} (U_{i+\frac{1}{2}}^{n,+} + U_{i+\frac{1}{2}}^{n,-}) - \frac{|C_{i+\frac{1}{2}}|}{2} (U_{i+\frac{1}{2}}^{n,+} - U_{i+\frac{1}{2}}^{n,-}) \tag{10}$$

$$C_{i+\frac{1}{2}} = x_{i+\frac{1}{2}}^n - x_{i+\frac{1}{2}}^{n+1} \\ U_{i+\frac{1}{2}}^{n,-} = U_i^n + \tilde{\psi}_i^n (x_{i+\frac{1}{2}}^n - x_i^n) \tag{11}$$

and

$$U_{i+\frac{1}{2}}^{n,+} = U_{i+1}^n - \tilde{\psi}_{i+1}^n (x_{i+1}^n - x_{i+\frac{1}{2}}^n) \tag{12}$$

Where $\tilde{\psi}$ is a slope limiter that can be defined in several ways [19, 20]. We use Eq. (9) to update the solution on new grids after each change of nodes position. It allows to take into account the conservation of the total mass of the solution on each interval I_i [2]. At every moment t^n we use the new positions of the nodes to define elementary volumes V_i^n on which the PDE of the problem will be integrated:

$$V_i^n =]x_{i-\frac{1}{2}}^n, x_{i+\frac{1}{2}}^n[\times [t^n, t^{n+1}] \tag{13}$$

More details on the moving mesh generation are given in [2].

3.2. PDE Discretization

The second step of the problem (Eq. (1)) resolution by the chosen method is to establish the

numerical scheme of this method that will compute the different values U_i^n of the unknown function U at node x_i and time t^n . The establishment of this scheme begins with a mandatory rewrite of the problem PDE in the form:

$$\frac{\partial U(x,t)}{\partial t} + \frac{\partial(\tilde{f}(U))}{\partial x} = 0 \tag{14}$$

With

$$\tilde{f}(U) = f(U) - \varepsilon \frac{\partial U(x,t)}{\partial x} \tag{15}$$

Then, this new form is integrated on each elementary volume V_i^n as follows:

$$\int_{t^n}^{t^{n+1}} \int_{x_{i-\frac{1}{2}}}^{x_{i+\frac{1}{2}}} \frac{\partial U(x,t)}{\partial t} dxdt + \int_{t^n}^{t^{n+1}} \int_{x_{i-\frac{1}{2}}}^{x_{i+\frac{1}{2}}} \frac{\partial(\tilde{f}(U))}{\partial x} dxdt = 0 \tag{16}$$

We get:

$$\frac{h_i^{n+1}}{h_i^{n+1}} \int_{x_{i-\frac{1}{2}}}^{x_{i+\frac{1}{2}}} U(x, t^{n+1}) dx - \frac{h_i^n}{h_i^n} \int_{x_{i-\frac{1}{2}}}^{x_{i+\frac{1}{2}}} U(x, t^n) dx + \int_{t^n}^{t^{n+1}} \left(\tilde{f}\left(U(x_{i+\frac{1}{2}}, t)\right) - \tilde{f}\left(U(x_{i-\frac{1}{2}}, t)\right) \right) dt = 0 \tag{17}$$

In Eq. (17), we have the average values of U^{n+1} and U^n on $]x_{i-\frac{1}{2}}^n, x_{i+\frac{1}{2}}^n[$.

These values are assigned to U_i^{n+1} and U_i^n :

$$U_i^{n+1} = \frac{1}{h_i^{n+1}} \int_{x_{i-\frac{1}{2}}}^{x_{i+\frac{1}{2}}} U(x, t^{n+1}) dx$$

and

$$U_i^n = \frac{1}{h_i^n} \int_{x_{i-\frac{1}{2}}}^{x_{i+\frac{1}{2}}} U(x, t^n) dx$$

We finally get the search numerical scheme known as high order finite volume method scheme:

$$U_i^{n+1} = \frac{h_i^n}{h_i^{n+1}} U_i^n - \frac{\tau}{h_i^{n+1}} \left(F\left(U_{i+\frac{1}{2}}^{n,-}, U_{i+\frac{1}{2}}^{n,+}\right) - F\left(U_{i-\frac{1}{2}}^{n,-}, U_{i-\frac{1}{2}}^{n,+}\right) \right) \tag{18}$$

Where

$$F\left(U_{i+\frac{1}{2}}^{n,-}, U_{i+\frac{1}{2}}^{n,+}\right) = \frac{1}{\tau} \int_{t^n}^{t^{n+1}} \tilde{f}\left(U(x_{i+\frac{1}{2}}, t)\right) dt \tag{19}$$

And

$$F\left(U_{i-\frac{1}{2}}^{n,-}, U_{i-\frac{1}{2}}^{n,+}\right) = \frac{1}{\tau} \int_{t^n}^{t^{n+1}} \tilde{f}\left(U(x_{i-\frac{1}{2}}, t)\right) dt \tag{20}$$

Eqs. (19) and (20) are respectively the average value of the flow that has passed through the $x_{i+\frac{1}{2}}^n$ and $x_{i-\frac{1}{2}}^n$ for the period $\tau = t^{n+1} - t^n$. They are approached by patterns that enable the convergence of Eq. (18).

$U_{i+\frac{1}{2}}^{n,-}$ and $U_{i+\frac{1}{2}}^{n,+}$ are defined by Eqs. (11) and (12).

$U_{i-\frac{1}{2}}^{n,-}$ and $U_{i-\frac{1}{2}}^{n,+}$ are defined in a similar way.

Finally, to get better accuracy in relation to the time, Eq. (18) is replaced by a second-order Runge-Kutta scheme:

$$\begin{cases} U_i^* &= U_i^n + \tau \Gamma_i(U^n) \\ U_i^{n+1} &= \frac{1}{2}(U_i^n + U_i^* + \tau \Gamma_i(U^*)) \end{cases} \tag{21}$$

Where

$$\Gamma_i(U^n) = -\frac{1}{h_i^{n+1}} \left(F\left(U_{i+\frac{1}{2}}^{n,-}, U_{i+\frac{1}{2}}^{n,+}\right) - F\left(U_{i-\frac{1}{2}}^{n,-}, U_{i-\frac{1}{2}}^{n,+}\right) \right)$$

The convergence of this method to solve this Burgers problem was guaranteed by the error evolution as highlighted in figures 5, 6 and 7.

4. Results and discussion

Figures 1 and 2 give respectively the exact solution for $t \in [0, 1]$ and its sections at times $t = 0, t = 0.2, t = 0.4, t = 0.6, t = 0.8$ and $t = 1$ (in a chosen unit).

Figures 3 to 5 show the numerical solution of the problem on Ω , its sections at indicated times and the mesh trajectories of 100 nodes, respectively. The parameters of the method which it used to calculate the numerical solution are given by: NS.st = 600, NT.st = 1500 and CPU.t = 36.4, where NS.st and NT.st are the number of nodes in Ω space interval and time interval, respectively. CPU.t is the period of the calculation.

The figure 6 helps to locate the position of the steep part of the solution over time and in particular the area where the solution passes from 2 steep parts to a much more steep parts. Figure 6 shows comparison between the numerical and

exact solutions. On the left side, U_{ex} and U_{num} are the exact and numerical solutions, respectively. On the right side, we have the graphical representation of the gap between the numerical and exact solutions for (NS.st, NT.st) = (100, 300).

In table 1, E_1 and E_2 are defined as follow:

$$E_1 = \|U_{ex} - U_{num}\|_{\infty}$$

And

$$E_2 = \|U_{ex} - U_{num}\|_2.$$

From the figures 5 and 6, we note that:

$$\lim_{(\Delta x, \Delta t) \rightarrow (0,0)} \|U_{ex} - U_{num}\|_2 = 0$$

and therefore, U_{num} gets closer to U_{ex} .

In figures 7 to 9, we have on the left, comparison between U_{ex} and U_{num} and, on the right, we have the representation of the gap between U_{ex} and U_{num} from the (NS.st, NT.st) = (100, 300), (NS.st, NT.st) = (300, 500) and (NS.st, NT.st) = (600, 1500). We can notice the progressive decrease of this gap.

Table 1

Error between the numerical solution and the exact solution.

Error/Times	t = 0.2	t = 0.4	t = 0.6	t = 0.8	t = 1
E_1	4.10^{-3}	4.10^{-3}	$9.1.10^{-3}$	$9.4.10^{-3}$	$9.4.10^{-3}$
E_2	$9.9.10^{-3}$	$1.1.10^{-2}$	2.10^{-2}	$2.1.10^{-2}$	$2.1.10^{-2}$

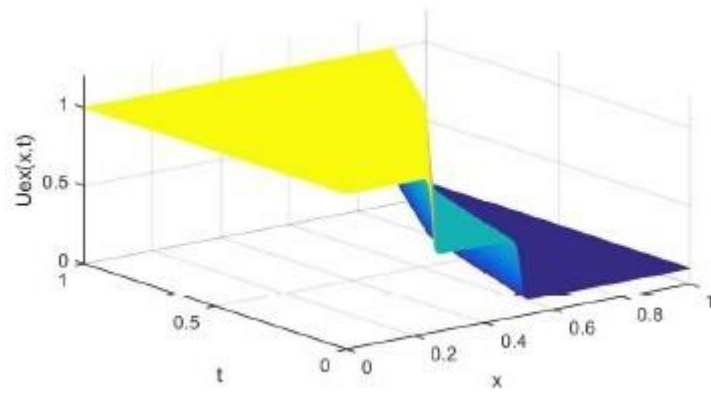


Fig. 1. Exact solution for $t \in [0, 1]$.

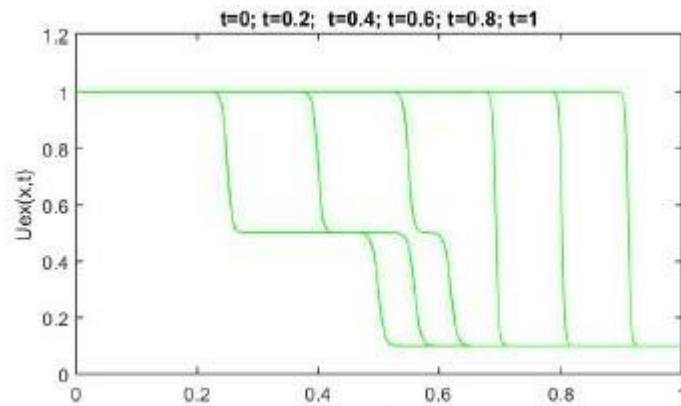


Fig. 2. Exact solution at times $t = 0, t = 0.2, t = 0.4, t = 0.6, t = 0.8$ and $t = 1$ (from left to right).

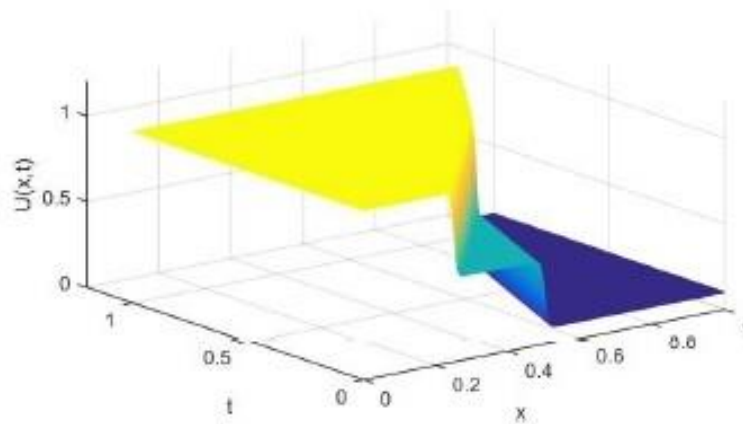


Fig. 3. Numerical solution computed with $N = 600$ and $\tau = \frac{1}{1500}$ for $t \in [0, 1]$.

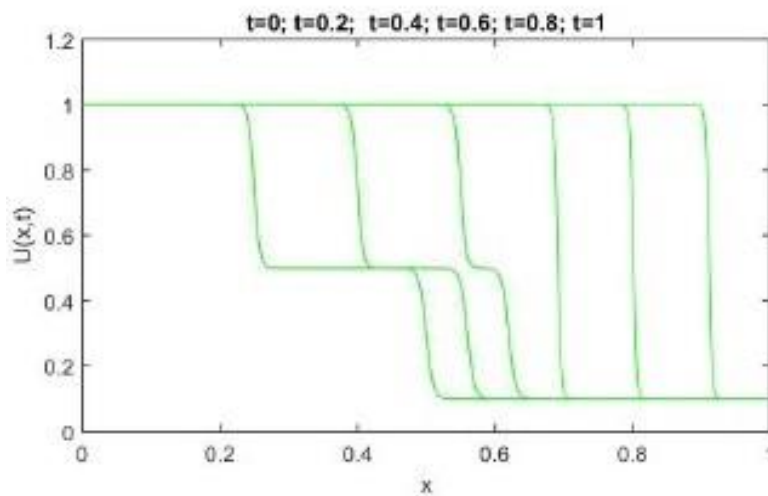


Fig. 4. Numerical solution computed with $N = 600$ and $\tau = \frac{1}{1500}$ at times $t = 0, t = 0.2, t = 0.4, t = 0.6, t = 0.8$ and $t = 1$ (from left to right).

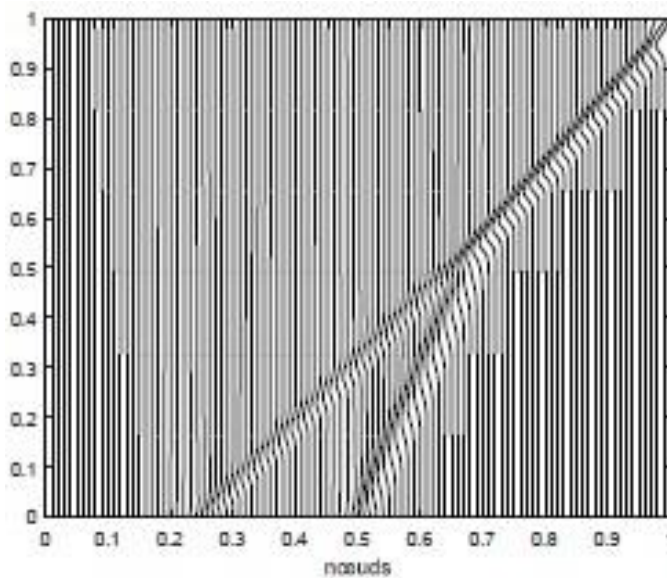


Fig. 5. Mesh trajectories.

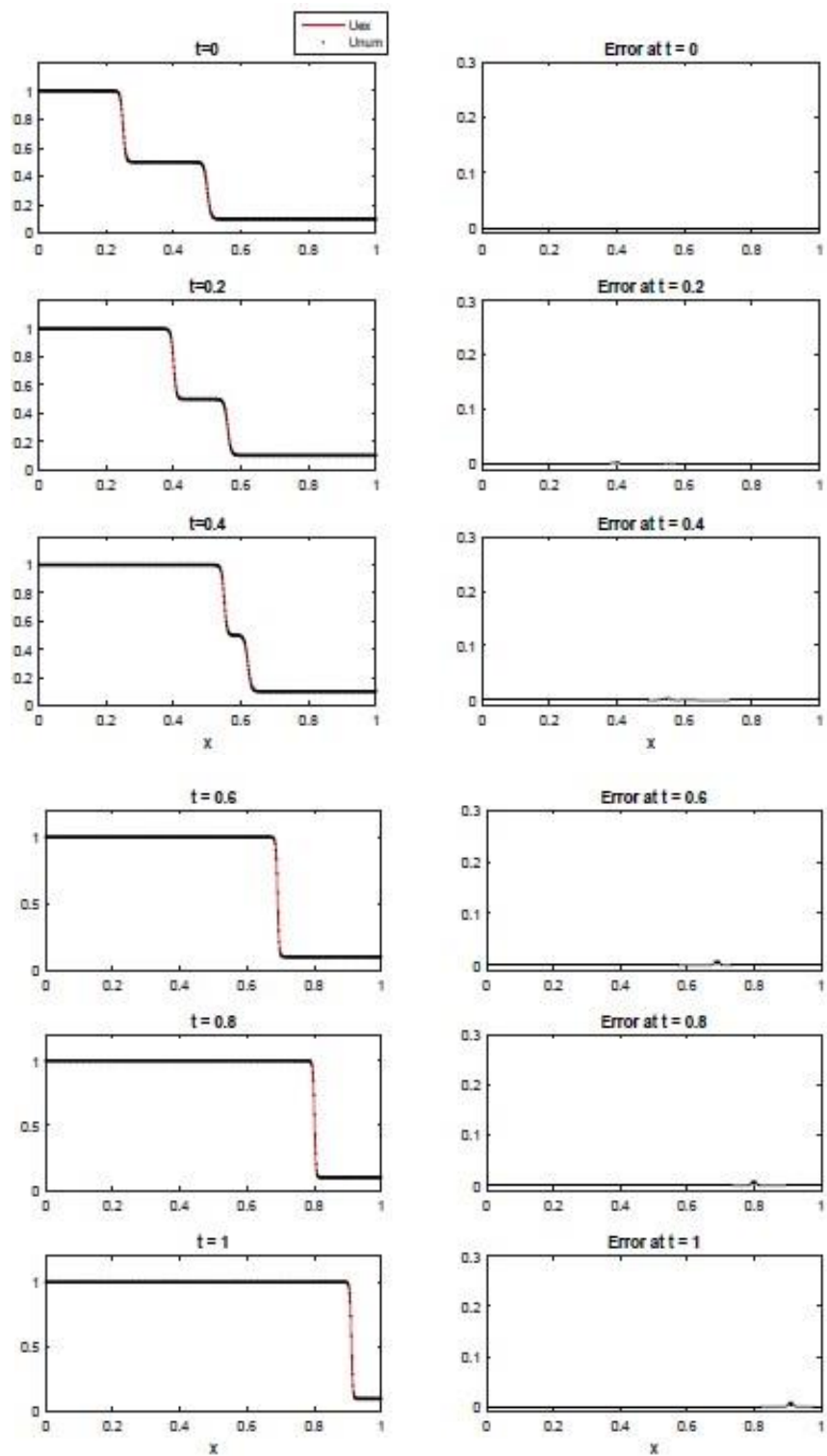


Fig. 6. Graphical comparison between the numerical and exact solutions.

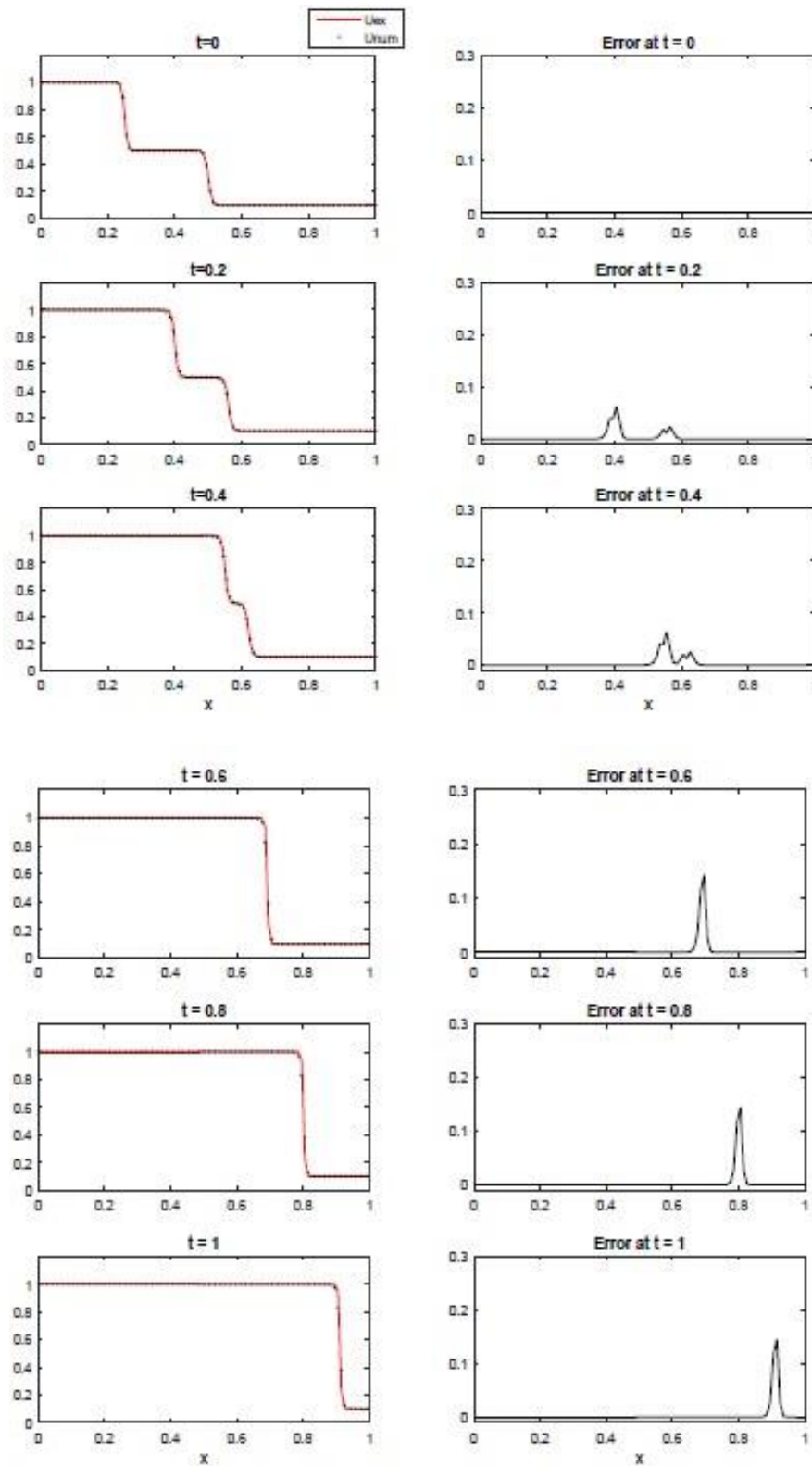


Fig. 7. Left: comparison between the numerical and exact solution. Right: error between the numerical and exact solutions for (NS.st, NT.st) = (100; 300).

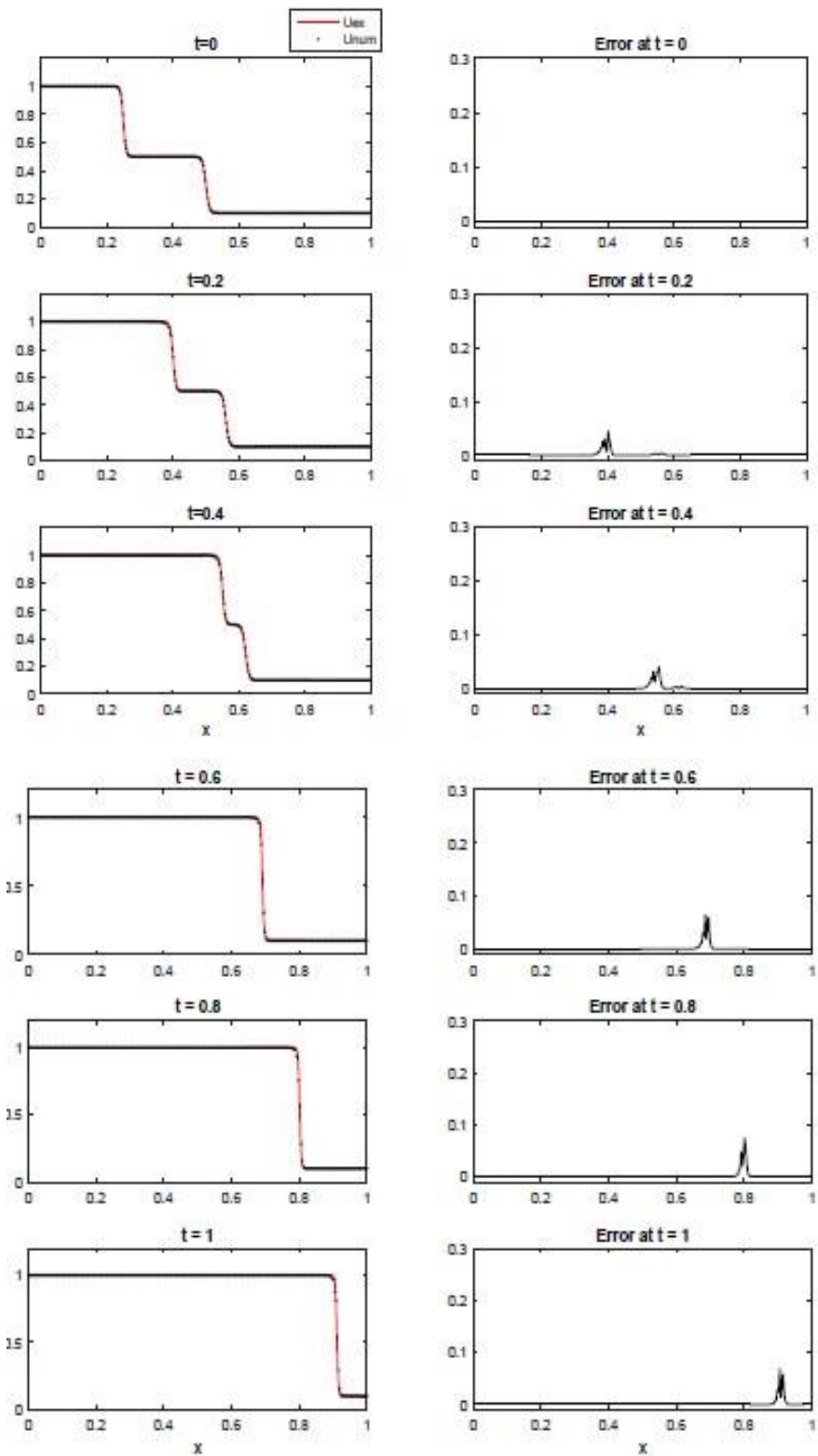


Fig. 8. Left: comparison between the numerical and exact solutions. Right: error between the numerical and exact solutions for $(NS.st, NT.st) = (300; 500)$.

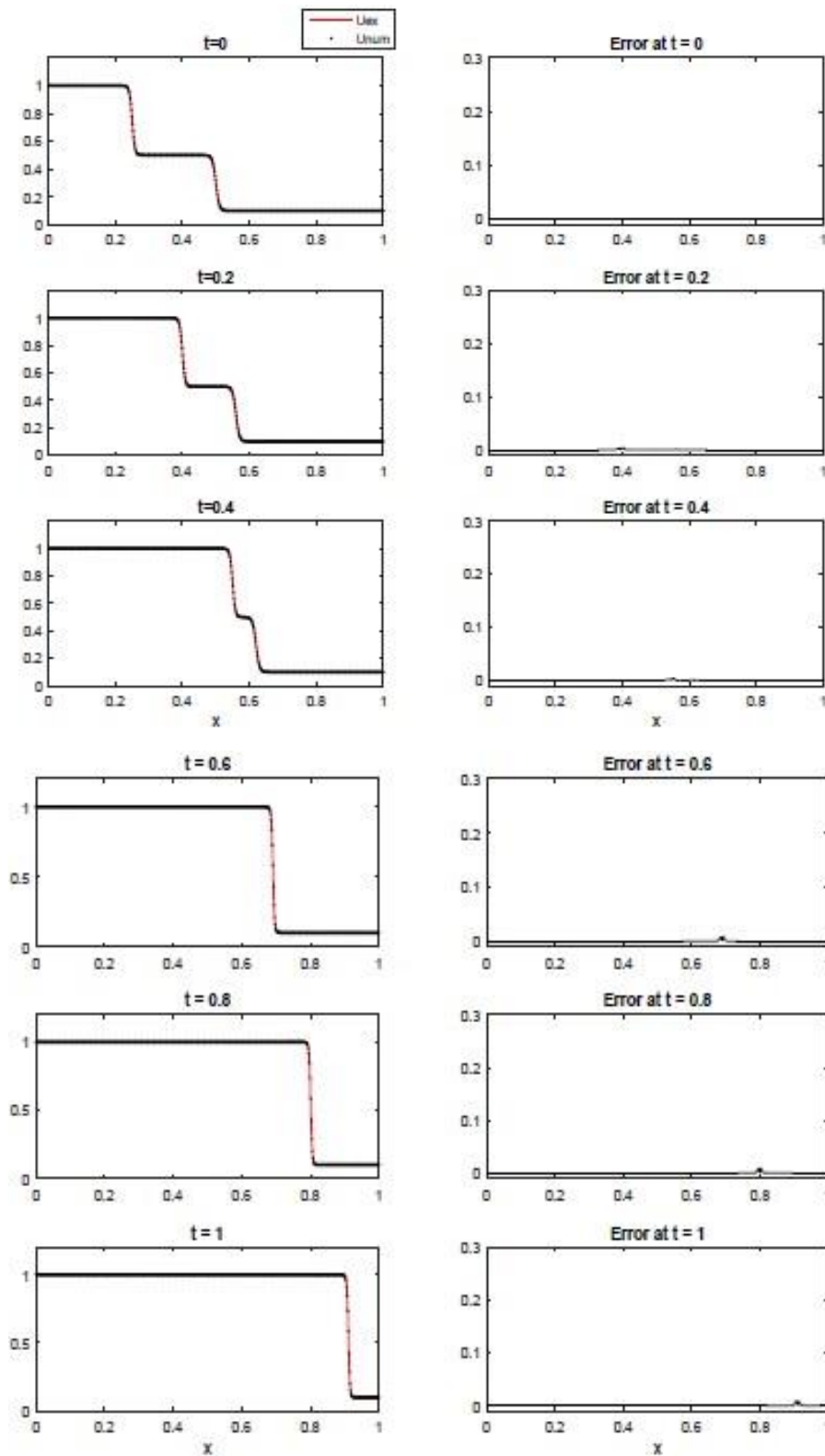


Fig. 9. Left: comparison between the numerical and exact solutions. Right: error between the numerical and exact solutions for $(NS.st, NT.st) = (600; 1500)$.

5. Conclusion

In this paper, we have briefly described the adaptive moving mesh finite volume method, before applying it to the resolution of the chosen test problem. Graphic comparisons between the exact solution and the numerical solution were carried out, before closing with the graphs making it possible to observe the evolution of the error according to the number of grid points. According to obtained results, we effectively notice that the adaptive moving mesh finite volume method has some advantages. The main advantages highlighted are the NS.st, NT.st, CPU.t and the numerical solution accuracy. Adaptive moving mesh methods offer a great possibility to improve the accuracy of numerical solution by continuing to increase the values of NS.st and NT.st. Therefore, the adaptive moving mesh finite volume method can be a best opportunity to numerically solve problems with PDEs which are hyperbolic conservation law with a small diffusion term. However, we note that the number of nodes at the origin of our results remains high compared to literature reports. This is linked to several reasons, some of which will be taken into account in our future experiments, in particular the Lagrangian form of the PDE of the problem.

References

- [1] Weizhang Huang, Robert D. Russell, *Adaptive moving mesh methods*, Springer, New York, XVII (2011).
- [2] Huazhong Tang, Tao Tang, *Adaptive mesh method for one- and two dimensional hyperbolic conservation laws*, SIAM J. Numer. Anal. 41(2) (2003) 487-515.
- [3] A. van Dam, *Moving meshes and solution monitoring for compressible flow simulation*, Ph.D. thesis, Mathematical Institute, Utrecht University, Netherlands (2009).
- [4] John M. Stockie, John A. Mackenzie, Robert D. Russel, *A Moving Mesh Method For One-Dimensional Hyperbolic Conservation Laws*, SIAM Journal on Scientific computing 22(5) (1999) 1791-1813.
- [5] J.A. Mackenzie, *Moving mesh finite volume methods for one-dimensional evolutionary partial differential equation*, Technical Report no. 96/32, Department of mathematics, University of Strathclyde (1996).
- [6] Fredrik Svensson, *Moving meshes and higher order finite volume reconstructions*, International Journal on finite volumes, Institut de Mathématiques de Marseille, AMU 3(1) (2006) 1-27.
- [7] B.N. Azarenok, *Variational barrier method of adaptive grid generation in hyperbolic problems of gas dynamics*, SIAM J. Numer. Anal. 40 (2002) 651-682.
- [8] B.N. Azarenok, S.A. Ivanenko, *Application of adaptive grids in numerical analysis of time-dependent problems in gas dynamics*, Comput. Math. Phys. 40 (2000) 1330-1349.
- [9] B.N. Azarenok, S.A. Ivanenko, T. Tang, *Adaptive mesh redistribution method based on Godunov's scheme*, Comm. Math. Sci. 1 (2003) 152-179.
- [10] Paul Andries Zegeling, *An Adaptive Grid Method for a Non-equilibrium PDE Model from Porous Media*, J. Math. Study July 48(2) (2015) 93-104.
- [11] Sean McDonald, *Development of a High-Order Finite-Volume Method for Unstructured Meshes*, Master of Applied Science thesis, Graduate Department of Aerospace Engineering, University of Toronto (2011).

[12] A. Harten, J. M. Hyman, *Self-adjusting grid methods for one-dimensional hyperbolic conservation laws*, J. Comput. Phys. 50 (1983) 235-269.

[13] P. Paul, B.Sc. Neary, Adaptive space meshing strategies for the numerical solution of parabolic partial differential in one space dimension, M.Sc. degree by research thesis, School of mathematical sciences, Dublin City University (1990).

[14] E.R. Benton, G.W. Platzman, *A table of solutions of the One-Dimensional Burgers Equation*, Quart. Appl. Math. 30 (1972)195-212.

[15] Longin Somé, Using an adaptive moving mesh lines method for numerical resolution of Partial Differential Equations modeling evolutionary phenomena, PhD thesis, Department of mathematics, Ouaga 1 Pr Joseph KI-ZERBO University, Burkina Faso (2007).

[16] Randall J. Leveque, *Nonlinear Conservation Laws and Finite Volumes Methods for Astrophysical Fluid Flow*, Springer-Verlag (1998).

[17] Randall J. Leveque, *Finite volume Methods for hyperbolic Problems*, Press Syndicate of the University of Cambridge (2002).

[18] R.M. Furzeland, J.G. Verwer, P.A. Zegeling, *A Numerical Study of Three Moving-Grid Methods for One-Dimensional Partial Differential Equations Which are Based on the Method of Lines*, Journal of Computational Physics 89 (1990) 349-388.

[19] Miroslav Cada, Compact third-order limiter functions for finite volume methods, Ph.D. Thesis, Dipl. Geo Physiker, Ludwig-Maximilians University, Munich (2009).

[20] Mamadou Ouédraogo, Longin Somé, Kassiénou Lamien, *Using some flux limiters methods to solve three test problems*, Far east journal of applied mathematics 93(2) (2015) 83-108.